Effect of Thermo-Physical Properties on Solidification Behavior of Large Size High Strength Steel Ingots

ZHANG Chunping[1], SHAHRIARI Davood[1], LOUCIF Abdelhalim[1], JAHAZI Mohammad[1], LAPIERRE-BOIRE Louis-Philippe[2], TREMBLAY Rami[2]

(1. École de Technologie Supérieur, 1100 Rue Notre-Dame Ouest, Montréal, Québec, H3C 1K3, Canada;
2. Finkl-Steel-Sorel, 100 Rue McCarthy, Saint-Joseph-de-Sorel, Québec, J3R 3M8, Canada)

Paper presented at
7th International Conference on Modelling and Simulation of Metallurgical Processes in Steelmaking (SteelSim 2017)
Qingdao, China, Aug. 16-17, 2017

Paper presented at
7th International Conference on Modelling and Simulation of Metallurgical Processes in Steelmaking (SteelSim 2017)
Qingdao, China, Aug. 16-17, 2017

Effect of Thermo-Physical Properties on Solidification Behavior of Large Size High Strength Steel Ingots

ZHANG Chunping[1], SHAHRIARI Davood[1], LOUCIF Abdelhalim[1], JAHAZI Mohammad[1], LAPIERRE-BOIRE Louis-Philippe[2] and TREMBLAY Rami[2]
(1. École de Technologie Supérieur, 1100 Rue Notre-Dame Ouest, Montréal, Québec, H3C 1K3, Canada;
2. Finkl-Steel-Sorel, 100 Rue McCarthy, Saint-Joseph-de-Sorel, Québec, J3R 3M8, Canada)

Abstract: The impact of different microsegregation models on solidification behavior of large size steel ingots was investigated. The microsegregation models include the ideal equilibrium solidification equation, the extreme Scheil-Gulliver, and the non-equilibrium equations. Different dendritic solidification equations were used to study the evolution of the properties and the cooling process of a 40 Metric Tons (MT) ingot of a medium carbon high strength steel. Material thermophysical properties were determined by means of thermodynamic softwares FactSage® together with various proposed models from the literature and the thermal simulations were done using Thercast® FEM code. The results obtained in this study demonstrate the significant influence of microsegregation model on temperature dependent solid fraction profiles, thermophysical properties, thermal field and solidification time needed for the casting of the large size ingot, which ultimately affect the extent of macrosegregation.
Key Words: steel, large size ingot, casting simulation, thermo-physical properties, equilibrium model, non-equilibrium models

Macrosegregation, as a compositional heterogeneity, is one of the most significant defects occurring during the solidification process. It exerts a determining effect on the properties of heavy ingots and has proved difficult to remove. For a broad understanding of the practical processes involving the formation and development of macrosegregation, computer simulation is the most economical and fastest approach. However, reliable prediction of concentration segregation during ingot casting greatly depends on the reliability and precision of the input parameters concerning solute redistribution in the solidification processes. The latter are determined by dendritic microsegregation models [1]. It is the microsegregation of elements on the dendritic scale which ultimately leads to enrichment of the liquid and macroscale advection of species. Therefore, the selection of the microsegregation model will have a direct impact on the outcome of any macrosegregation prediction tool.

The objective of the present work is to investigate the effect of microsegregation model selection on temperature dependent solid fraction profiles, thermophysical properties and solidification behavior of a medium-carbon high strength steel. For this, notable analytical or semi-analytical treatments of solute redistribution problem were summarized, including the ideal equilibrium lever-rule equation [2], the extreme non-equilibrium Scheil-Gulliver treatment [3], as well as other microsegregation models presented by Brody Flemings [4], Clyne and Kurz [5], Kobayashi and Ohnaka [6], respectively. These microsegregation models were applied to determine thermophysical properties of the steel using thermodynamic softwares FactSage® [7], together with various proposed models from the literature. Three-dimensional thermic simulations of the solidification process of a 40MT steel ingot were performed using Thercast® 8.2 version FEM code [8] with casting parameters selected according to the actual industrial operational conditions.

1 Microsegregation models

In the dendritic solidification process, solute diffusion in the liquid, which is at the origin of microsegregation, is complete. Hence, interdendritic microsegregation models are formulated by dealing with the diffusion in the solid phase, described by the relationship between the solute concentration at the growth solid/liquid interface C_S and the solid fraction f_S. Solute diffusion in the solid depends on the value of the dimensionless back-diffusion Fourier number α [5]:

$$\alpha = D_S(t_f / L^2) \quad (1)$$

where D_S is the solute diffusivity in the solid, t_f is the diffusion time (local solidification time) and L is the diffusion distance (half of the dendrite spacing λ).

If $\alpha >> 1$, the diffusion is assumed to be so intense that the composition is always uniform within each phase (i.e. the system is always in thermodynamic equilibrium), then the solidification behavior is described by the classical lever rule written as $C_S = kC_0 / \{(1-f_S) + kf_S\}$, predicting the changing composition of the solid at the solid/liquid interface during solidification [2]. Here, C_0 is the original composition, and k is the partition coefficient. The above equation can also be expressed as the variation of the local solid fraction f_S in terms of the system temperature:

$$f_S = \{1/(1-k)\}\{(T_L - T)/(T_f - T)\} \quad (2)$$

where T_L is the liquidus temperature, T_f is the melting temperature for pure iron.

If α << 1, the diffusion in the solid can be ignored. Then a complementary limit case to the lever rule can be used, i.e. $C_S = kC_0(1-f_S)^{k-1}$, or again expressing the local solid fraction at a temperature [3]:

$$f_S = 1-\left\{(T_f - T)/(T_f - T_L)\right\}^{1/(k-1)} \quad (3)$$

which is often referred to as the Scheil-Gulliver or Scheil equation.

The actual freezing behavior, however, is expected to lie somewhere between the above two extremes, depending on the importance of solid state diffusion. Therefore, various models have been put forward to quantify the effect of solid state diffusion for the intermediate states between the Scheil and lever rule cases. Under these conditions, the following assumptions are made for the analysis [5]: straight liquidus and solidus lines of the concerned phase diagram (i.e. a constant partition coefficient *k*), a constant diffusion coefficient, a plate-like or cylindrical dendrite geometry, a single phase in the solid (an abrupt occurrence of δ-ferrite/γ-austenite transformation), and a parabolic ($V = \sqrt{t/t_f}$) or linear local solid/liquid interface advance velocity ($V = L/t_f$).

Brody and Flemings were the first to analyze the solid state diffusion based on a one-dimensional solute redistribution model and presented $C_S = kC_0\left\{1-(1-2\alpha k)f_S\right\}^{(k-1)/(1-2\alpha k)}$ of a decreasing parabolic behavior for the solid/liquid interface advance [4]. The above equation can also be expressed as:

$$f_S = \left[1/(1-2\alpha k)\right]\left\{1-\left[(T_f - T)/(T_f - T_L)\right]^{(1-2\alpha k)/(k-1)}\right\} \quad (4)$$

Clyne and Kurz modified the Brody-Flemings model by introducing a parameter, $\Omega(\alpha)$, to be substituted for α in Eq.(4) to limit the errors introduced by the geometrical simplifications involved in the Brody-Flemings model [5]:

$$\Omega = \alpha\left\{1-\exp(-1/\alpha)\right\} - (1/2)\exp\left\{-1/(2\alpha)\right\} \quad (5)$$

Kobayashi proposed an extended mathematical model, incorporating a thermal model of solidification into the analysis, and solved more rigorously Brody-Flemings model with parabolic growth. His equation was found to coincide with the equation derived by Ohnaka on the basis of a profile method [6] $C_S = kC_0\left\{1-\left[1-2\alpha k/(1+2\alpha)\right]f_S\right\}^{\eta}$ and:

$$f_S = \left[(1+2\alpha)/(1+2\alpha-2\alpha k)\right]\left\{1-\left[(T_f - T)/(T_f - T_L)\right]^{1/\eta}\right\} \quad (6)$$

$$\eta = (k-1)(1+2\alpha)/(1+2\alpha-2\alpha k) \quad (7)$$

2 Material and methods

The composition of the investigated steel is listed in Table 1. Typical thermophysical data including the liquidus temperature (1492°C), partition coefficients k_δ (0.82) and k_γ (0.4053) as well as the δ/γ phase transformation temperatures (1478°C) were determined by means of the computational thermodynamics program FactSage® version 7.0 [7].

It was assumed that the primary dendrite arm spacing λ_1 is equal to the secondary dendrite arm spacing λ_2. Hence, the Fourier number α was determined via the empirical expression for low-alloyed steels relating the secondary dendrite arm spacing λ_2 (in μm) to the constant cooling rate $\dot{T}$ (in °C/s) and the local solidification time t_f (in s) [9]:

$$\lambda_2 = 150\dot{T}^{-0.385} = 150\times((T_L - T_S)/t_f)^{-0.385} \quad (8)$$

where T_S is the solidus temperature in °C.

The temperature dependence of the effective thermal conductivity K_{th}, specific heat capacity C_P and density ρ of the heterogeneous mixture of δ-ferrite, γ-austenite and liquid in the mushy state of the studied medium carbon high strength steel was calculated with the volume fractions and properties of each phase in the mushy state from the equations in reference [10] for density and [11] for thermal conductivity and specific heat, respectively.

The thermal simulations of the solidification process of a 40 MT ingot were performed in the finite element code Thercast® with a maximum temperature of 800 °C as the stop signal to make sure that solid state is achieved at the center of the large size ingot. All the details of the models can be found in references [12, 13].

Table 1 Chemical composition of the investigated steel (wt.%)

C	Mn	P	S	Si	Ni	Cr	Mo	Cu
0.35	0.82	0.007	0.002	0.4	0.15	1.79	0.46	0.13

3 Results and discussions

3.1 Effect of microsegregation models on solid fraction profiles

An indication of the determination of Fourier number α for the steel based on Eq. (1) is given in Table 2, where the diffusivity (in $\mu m^2/s$) of carbon in austenite is taken as a mean diffusivity over the freezing interval from the expression [14]:

$$D_s(m^2/s) = 0.1\times10^{-4}\times\exp(-16321.9/T(K)) \quad (9)$$

Here, only the segregation of carbon is considered. Three cases of dendritic arm spacings were investigated, and assumed to be representative of the

structure's size of the ingot wall side, radial midway, and the center. It was found that α values tend to increase from the ingot wall side chill zone to the center. This corresponds to the increase of the dendritic arm spacing and then local freezing time from the surface to the center.

Table 2 Calculated solidification parameters for the current steel

λ_2 (μm)	t_f (s)	α
2	0.0009	0.616
20	0.36	2.44
200	142	11.27

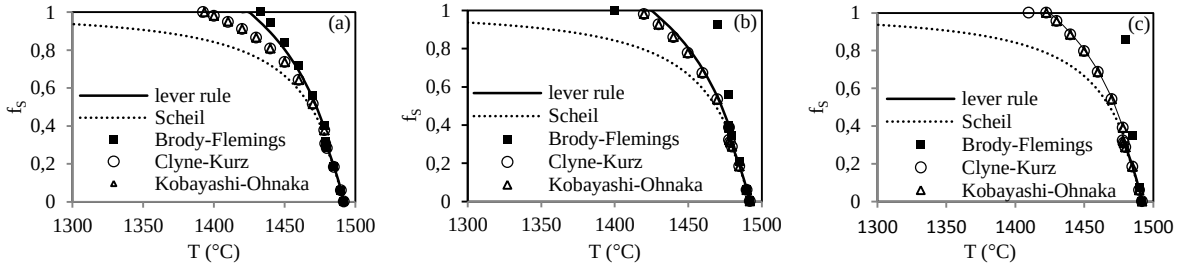

Fig.1 Predicted solid fraction/temperature curves for the investigated steel according to the classical limiting cases and the proposed models over a range of Fourier number values
a—α = 0.616; b—α = 2.44; c—α = 11.27

Figure 1 shows the dependence of local solid fraction within the mushy zone on local temperature for the steel over the investigated range of Fourier number values according to different models (Eqs. (2-7)). It is clear that large values of α lead to physically impossible curves predicted by Brody-Flemings in that the temperature at which solidification is complete lies above the equilibrium solidus. Similar errors predicted by Brody-Flemings equations have also been reported by others [5, 6]. It appears probable that the approximate equations derived by Brody-Flemings cannot be directly applied to large ingot cases. In contrast, the predictions made using Clyne-Kurz and Kobayashi-Ohnaka equations are similar. The latter two models may be regarded as better approximation for the diffusion behavior in the solid. Examination of Figure 1 also reveals that as α is increasing from 0.616 (Fig. 1(a)) to 11.27 (Fig. 1(c)), solute redistribution in the solid phase progressively becomes rather close to the lever rule. All the changes arose after the δ/γ transformation occurrence during the cooling process.

3.2 Effect of microsegregation models on thermophysical properties and solidification behavior

Figure 2 shows the variation of material dynamic thermophysical properties as a function of local solid fraction in the mushy zone. Temperature dependent material thermophysical behaviors are found to be significantly influenced by dendritic solidification models.

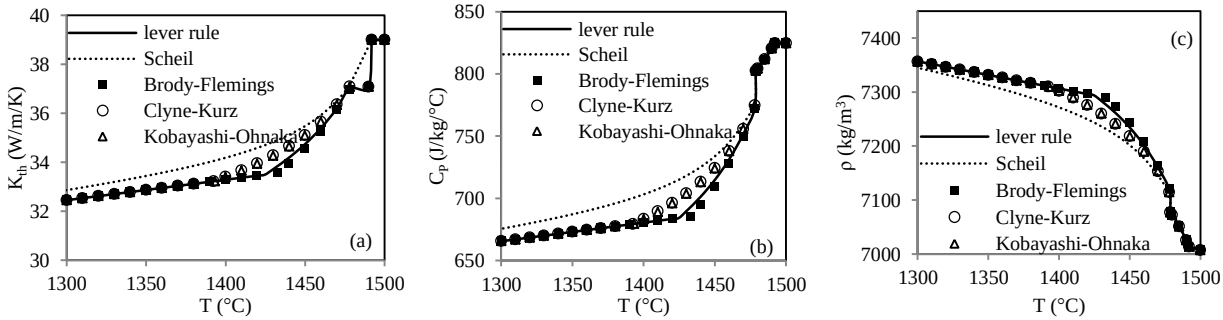

Fig.2 Temperature dependence of physical properties for the steel in study according to different microsegregation solidification models for the case α = 0.616
a—thermal conductivity; b—specific heat; c—density

When different thermophysical properties were used for thermal field computation of the solidification process, it was found that temperature distribution and solidification times correlate with the microsegregtation models, as seen in Figures 3 and 4. Kobayashi-Ohnaka and Scheil models gave rise to distinctive higher thermal gradients than the classic equilibrium rule. Such higher thermal gradients could be responsible for the formation of channel segregates during the cooling process. In

addition, the occurrence of less solute diffusion in solid resulted in higher ingot cooling times, passing from about 11 hours 48 minutes for complete solute redistribution determined by the lever rule to 29 hours 18 minutes for no solute diffusion in solid after Scheil mode. These findings indicate that the latter two models would predict slower solidification process, leaving enough time for the solute-rich interdendritic liquid to redistribute in the ingot, aggravating macroscopic solute segregation.

It should be noted that the empirical relationships used in this work (Eq.(8)) refer to secondary arm spacing measurements. But, the choice of dendritic arm spacing is rather uncertain, although it should probably lie somewhere between the primary and secondary spacings. In general, primary arm spacing is higher than the secondary arm spacing so that the calculated extent of diffusion would constitute a lower limit in this regard. Therefore, further work will focus on experimental microsegregation characterization to test the validity of the proposed microsegregation models and the empirical relationships used to calculate the Fourier number for the purpose to apply the analysis results to macrosegregation modeling.

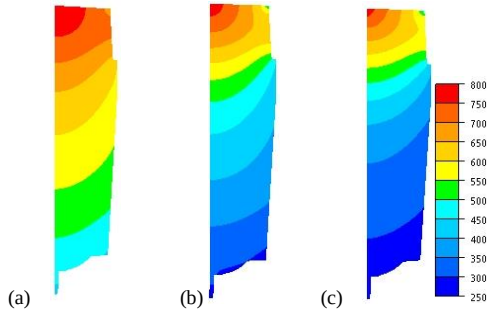

Fig.3 Temperature distribution (°C) of the thermic simulation with the stop condition of 800°C after different microsegregation models
a—lever rule; b—Kobayashi-Ohnaka (α = 0.616); c—Scheil

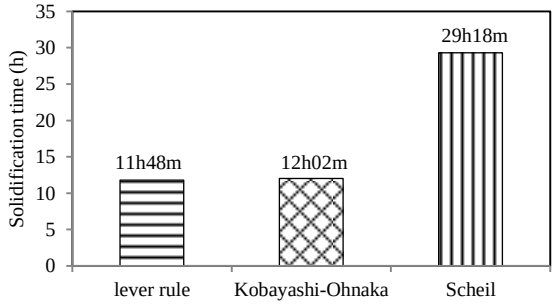

Fig.4 Total solidification time (s) for thermic simulations stopping at 800 °C as the maximum temperature based on microsegregation models of lever rule, Kobayashi-Ohnaka (α = 0.616) and Scheil.

4 Conclusions

(1) Microsegregation model selection can significantly influence the prediction of the local solid fraction within the mushy zone.

(2) For large size steel ingot, solidification behavior next to the chill zone are close to an intermediate state between the extreme lever rule and Scheil equations, while the central part behaves approximatively in the equilibrium state.

(3) For the investigated microsegregation models, Brody-Flemings approximation appears not applicable for large ingot cases; Clyne-Kurz and Kobayashi-Ohnaka models can predict similar results, which may be regarded as better approximation for the diffusion behavior in the solid.

Acknowledgement:

The financial support from the Natural Sciences and Engineering Research Council (NSERC) of Canada in the form of a Collaborative Research and Development Grant (CRDG) under number 470174 is gratefully acknowledged. Finkl Steel Co. is greatly appreciated for providing the material.

References:

[1] Fridberg J., Torndahl L. E., Hillert M.. Diffusion in Iron [J]. Jernkont Ann, 1969, 153: 263~276
[2] Smith W. F.; Hashemi, J.. Foundations of Materials Science and Engineering [M]. 4th ed. McGraw-Hill, 2006
[3] Scheil E., Metallk Z.. Bemerkungen zur Schichtkristallbildung, 1942, 34:70~72
[4] Flemings M.C.. Solidification Processing [J]. Metall Trans, 1974, 5(10): 2121~2134
[5] CLyne T.W., Kurz W.. Solute Redistribution during Solidification with Rapid Solid State Diffusion [J]. Metall Trans A, 1985, 12: 965~971
[6] Kobayashi S.. A Mathermatical Model for Solute Redistribution during Dendritic Solidification [J]. Trans ISIJ, 1988, 28: 535~542
[7] Bale C. W.. Macro Processing Manual, CRCT. 2017
[8] Thercast User Manual, France: Transvalor, 2012
[9] Suzuki A., Suzuki T., Nakaoka Y., et al. Nippon Kinzoku Gakkaishi. J Jpn Inst Met [J]. 1968, 32: 1301~1305
[10] Miettinen J., Louhenkilpi S.. Calculation of Thermophysical Properties of Carbon and Low Alloyed Steels for Modeling of Solidification Processes [J]. Metall Mater Trans, 1994, 25B: 909~916
[11] Meng Y., Thomas B. G.. Heat-transfer and Solidification Model of Continuous Slab Casting: CON1D [J]. Metall Mater Trans, 2003, 34B(5): 685~705
[12] Shahriari D., Loucif A., Jahazi M., et al. 3D Numerical Simulation of Solidification of Large Size Ingots of High Strength Steel. SteelSim 2015.
[13] Zhang C., Shahriari D., Loucif A., et al. Effect of Segregated Alloying Elements on the High Strength Steel Properties: Application to the Large Size Ingot Casting Simulation. TMS 2017 146th Annual Meeting & Exhibition Supplemental Proceedings, 2017, 491~500
[14] Gorni A. A. SP. S.V. Steel Forming and Heat Treating Handbook [M]. 2015, Brazil.